



1 The Potamochemical symphony: new progresses in the high 2 frequency acquisition of stream chemical data

3 Paul Floury^{1,2*}, Jérôme Gaillardet¹, Eric Gayer¹, Julien Bouchez¹, Gaëlle Tallec²,
4 Patrick Ansart², Frédéric Koch³, Caroline Gorge¹, Arnaud Blanchouin², and Jean-Louis
5 Roubaty¹

6 ¹ Institut de Physique du Globe de Paris, CNRS and Sorbonne Paris Cité, 1 rue Jussieu, 75238 Paris,
7 France

8 ² UR HBAN, Institut national de recherche en sciences et technologies pour l'environnement et
9 l'agriculture, Antony, France

10 ³ Endress+Hauser SAS, Huningue, France

11 Corresponding author. E-mail: floury@ipgp.fr

12

13 Abstract

14 Our understanding of hydrological and chemical processes at a catchment scale is
15 limited by our capacity to record the full breadth of the information carried by river
16 chemistry, both in terms of sampling frequency and in precision. Here, we present the
17 proof-of-concept of a new system of water quality monitoring that we called the “River
18 Lab” (RL), based on the idea of permanently installing a suite of laboratory instruments
19 in the field. Confined in a bungalow next to the river, this set of instruments performs
20 analyses at a frequency of 40-minutes for major dissolved species (Na^+ , K^+ , Mg^{2+} , Ca^{2+} ,
21 Cl^- , SO_4^{2-} , NO_3^-) through continuous sampling and filtration of the river water using
22 automated ion chromatographs. The RL was deployed in the Orgeval Critical Zone
23 Observatory, France for over a year of continuous analyses. Results show that the RL is
24 able to capture long-term fine chemical variations with no drift and a precision a
25 significantly better than conventionally achieved in the laboratory (up to ± 0.5 % for all
26 major species for over a day and up to 1.7 % over two months).



27 Using chemical signals obtained as a benchmark, we assess the effects of a lower
28 sampling frequency (typical of traditional field sampling campaigns) and of a lower
29 precision (typically reached in the laboratory) on the chemical river signal. The RL is
30 able to capture the abrupt changes in dissolved species concentrations during a typical
31 6-days flood event, as well as unexpected daily oscillations during a hydrological
32 ‘boring’ period of summer drought.

33 The unprecedented, high-resolution, high precision measurements made possible by the
34 RL open new perspectives for understanding critical zone hydro-bio-geochemical
35 cycles. This approach also offers a solution for operational agencies to monitor the
36 water quality in quasi real-time.

37

38 **1 Introduction**

39 River chemistry offers a window into the multiple processes that control the nature and
40 the abundance of solutes in continental waters and thus represents a tool to study the
41 Critical Zone (Neal et al. 2013; Calmels et al. 2011; Feng et al., 2004; Kirchner et al.,
42 2000; Kirchner et al., 2001; Neal et al., 2012). Moreover, understanding the parameters
43 that control river water geochemistry is one of the major challenges for humanity to
44 access and preserve drinkable water (Bain et al., 2012; Banna et al., 2013; Bartam and
45 Ballance, 1996), but our understanding is limited by the temporal resolution of sampling
46 (Whitehead et al., 2009). As summarized by J. Kirchner: “If we want to understand the
47 full symphony of catchment hydrochemical behaviour, then we need to be able to hear
48 every note.” (Kirchner et al., 2004). Yet, taking high-frequency sample sets back to the
49 laboratory is limited by the requirement of considerable human resources (Danielsen et
50 al., 2008; Rozemeiler et al., 2014; Strobl and Robillard, 2008; Telci et al., 2009;
51 Chapman et al., 1996; Halliday et al., 2015).



52 Thus far, high-frequency chemical measurements in catchments have been mostly
53 reported during short periods such as a single storm events or a day (Chapman et al.,
54 1997; Morel et al., 2009; Takagi et al., 2015; Nimick et al., 2011; Beck et al., 2009;
55 Brick et al., 1996; Kurz et al., 2013; Nimick et al., 2005; Gammons et al., 2007;
56 Montety et al., 2011; Neal et al., 2002; Tercier-Weaber et al., 2009; Liu et al., 2007).
57 These studies highlight the wealth of information provided by sampling at sub-hourly
58 frequency, however, such strategies underestimate the legacy of past hydrological
59 episodes (Kirchner 2006; Jasechko et al., 2016).

60 To date, the best combination of high frequency and long term monitoring ever reported
61 for river chemistry is a 7-hourly frequency sampling over 18 months (Neal et al., 2012).
62 This study demonstrated the “act of discovery” permitted by such sampling schemes,
63 but also highlights the practical limits of “manual approaches”. However, automated
64 approaches, developed using probes installed directly in the river (Rozemeijer et al.,
65 2010a; Macintosh et al., 2011; Cassidy and Jordan 2011; Dabakk et al., 1999; Glasgow
66 et al., 2004; Zhu et al., 2010; Yang et al., 2008) or online instrumental devices in which
67 continuously pumped water is injected (Rozemeijer et al., 2010b; Zabiegala et al., 2010;
68 Jordan and Cassidy 2011) have been demonstrated as a novel alternative to monitor
69 water chemistry. Thus far, these systems have only been applied to nutrients such as
70 dissolved N or P (Kunz et al., 2012; Clough et al., 2007; Aubert et al., 2013a; Aubert et
71 al., 2013b).

72 In this paper, we present a novel apparatus designed to bring the chemical laboratory to
73 the field: the River Lab (RL). This approach overcomes traditional limitations on the
74 number of samples and avoids several issues related to sample transport, filtration and
75 storage (von Freyberg et al., In review). RL prototype is one of the work packages of
76 the French program CRITEX: “Innovative sensors for the Temporal and spatial



EXploration of the CRITical Zone at the catchment scale”. The breakthrough of the RL lies in its ability to perform a complete chemical analysis of all inorganic major anionic and cationic species in the dissolved load of river water using ion chromatography (IC), to a frequency of up to one complete measurement every 40 minutes.

This article describes the analytical design of the RL and its performance by evaluating the precision, reproducibility and accuracy of concentration measurements. The first results from the RL reveal a significant improvement in reproducibility compared to conventional sampling and analysis techniques. Leveraging these optimal analytical conditions, the RL is able to reveal unsuspected temporal patterns of river chemistry, such as daily concentration variations. Thus, the RL opens new opportunities in the field of river chemistry research and operational monitoring.

88

2 Monitoring site

The RL was installed on the Orgeval river, a Critical Zone Observatory located 70 km eastward from Paris, France. The Orgeval is a temperate agricultural catchment, within the Seine river watershed, and is part to the French Critical Zone Observatory network RBV (“Réseau des bassins versants”). This catchment is one of the most instrumented and documented river observatories in France, with 50 years of hydrological data (Garnier et al., 2014). Catchment hydrologic data are available on the ORACLE website (<https://bdoh.irstea.fr/ORACLE/>).

The RL is installed at the outlet of the Avenelles river, a sub-catchment in the Orgeval watershed, which drains an area of 45 km². The climate is temperate and oceanic, with cool winters (mean temperature 3°C), warm summers (20°C in average) and a mean annual precipitation rate of ~ 650 mm. The Avenelles sub-catchment sits within the sedimentary carbonate-dominated Paris Basin. The river is perennial, supplied by



groundwater from the Brie aquifer, with a water chemistry dominated by Ca^{2+} , SO_4^{2-} , HCO_3^{2-} and NO_3^- ions. The water level at the Avenelles gauging station shows an average daily volumetric flow rate of $0.2 \text{ m}^3/\text{s}$ (from 1962 to 2016) with low water period in summer ($0.01 \text{ m}^3/\text{s}$) and flash flood events reaching $10.4 \text{ m}^3/\text{s}$ in spring.

106

107 **3 Design of the River Lab**

The concept of the RL is to pump river water and feed a set of physico-chemical probes and ion chromatography instruments (IC) for a complete analysis of major dissolved species continuously at high frequency (40 minutes for a complete analysis). All the instruments of the RL fit into an isolated bungalow of 4 m length by 2.5 m width, kept at $24^\circ\text{C} \pm 2^\circ\text{C}$. The RL was conceptualized by IPGP and IRSTEA and assembled by Endress & Hauser (E+H®).

114

The RL has been designed around a primary circuit, which pumps the river water at 700 liters per hour. First, the unfiltered river water sampled in the middle of the stream (Fig. 1) continuously supplies an overflow tank where 6 parameters are measured: pH, conductivity, dissolved O_2 , dissolved organic carbon (DOC), turbidity and temperature. The water is then released into the river downstream from the RL. The turnover time of water in this primary circuit is 2 minutes. The turbidity probe is installed upstream of the overflow tank in a pipe perpendicular to the flow to provide more accurate measurements. The turbidity and DOC probes benefit from an automatic self-cleaning each 5 minutes using compressed air. For all probes, the frequency of acquisition is one measurement per minute. The tank and each probe are hand-cleaned weekly. All information about characteristics and calibration for each probe are available as supplementary information “SI Probes characteristics”.



127 Second, a fraction of water pumped through the primary circuit feeds another circuit
128 directed toward two IC instruments for the measurement of major dissolved species
129 concentrations. A filtration system is deployed between the primary circuit and the IC
130 instruments, consisting of a tangential filter with a 2 μm pore size, followed by a 0.2 μm
131 frontal filtration system through cellulose acetate filters (Fig. 1) crucial for the IC
132 instruments. Cation and anion chromatographs, connected in series, are fed
133 simultaneously every 40 minutes from the filtered water circuit through a injection
134 valve. Between two injections, the water in the filtered circuit is constantly renewed (1
135 L per hour).

136 The IC analysis is performed using two Dionex[®] ICS-2100 (Thermo Fisher Scientific[®])
137 instruments using eluent produced with concentrated eluent cartridges and ultra-pure
138 water (Fig. 1). The cationic species measured are Na^+ , K^+ , Mg^{2+} and Ca^{2+} , while anionic
139 species are Cl^- , NO_3^- and SO_4^{2-} . The chosen analysis time is 30 minutes (40 minutes if
140 Sr^{2+} concentration measurements are included; see details in SI “Ion Chromatographs
141 characteristics”). The multiport valve installed upstream of the ICs allows us to check
142 the drift of the instruments and the background signal by regular introduction of
143 calibration solutions and pure distilled (see section 4). Both cationic and anionic
144 chromatographs are calibrated every two months using synthetic solutions mimicking
145 the river chemistry, made from 1000-ppm mono-elemental standard solutions. Two sets
146 of calibration solutions are prepared, one for anions and the second for cations. The first
147 solution (called “River x1”) is prepared based on concentrations of the river water
148 during summer, i.e. with the highest measured concentrations for most species. In the
149 second solution, these concentrations are doubled (called “River x2”). Further solutions
150 are produced out of River x1 and x2 through dilution by up to ten fold to achieve lower
151 concentrations (“River x0.5; x0.25; x0.1”). The resulting five calibration solutions cover



152 the entire range of possible natural variability of each species observed for the Orgeval
153 river, including flood events.

154

155 Data from probes and ICs are collected, merged and updated in a single database in real
156 time. Data from the gauging station (flow discharge and precipitation level) are
157 automatically added to the database. Several parameters of the RL can be remotely
158 monitored such as pump activity, pressure, flow and temperature in the primary circuit;
159 activation of the tangential filtration cleaning system, instrument connection, and
160 temperature in the bungalow. A set of alarms and sensors controls each key point of the
161 system. An email is automatically sent in case of dysfunction. Under normal operating
162 conditions, the RL needs human intervention only once per week.

163

164 **4 Performances of the River Lab**

165 RL data acquisition started on the 12th of June 2015. The reliability of the system was
166 assessed through 5 different tests involving IC measurements and the sampling
167 procedure (accuracy, drift, precision of the whole system, cross-contamination and
168 reproducibility). We refer to the 3rd edition of JCGM 200-2012 (JCGM 2012) for the
169 terminology used in assessing the performance criteria.

170

171 **4.1 Accuracy and instrumental drift**

172 The aim of the RL is to achieve very high frequency measurements of river chemistry
173 over long periods of time (pluriannual). To compensate for any long-term drift in the IC
174 calibration, instruments are calibrated with a new set of solutions every two months or
175 after each maintenance operation on the IC instruments. However, calibration drift can
176 occur over timescales shorter than two months, resulting in systematic and / or random



177 errors in concentration measurements. Using a set of injections of the “River x1”
178 solutions, over one week and over two months, we evaluated this effect (Table 1). For
179 all species measured, no systematic variation was observed in the measured
180 concentration of the solution “River x1”, showing that at the two timescales,
181 instrumental drift does not induce any systematic bias on concentration measurements,
182 and that most of the error is of a random nature. Therefore, the standard deviation of the
183 concentration measurement can be used as a reliable measure of the error due to
184 instrumental drift. The measurement error over one week is calculated as the standard
185 deviation of concentration measurements over 19 injections of solution “River x1”
186 performed every 8 hours during one week (from the 5th to the 12th of November 2015).
187 The measurement error over two months is calculated as the standard deviation of
188 concentration measurements over a series of injections performed every two days
189 during two months (from the 28th December 2015 to the 26th February 2016). These
190 error estimates are better than 1 % over one week and better than 1.7 % over two
191 months (Tab. 1).

192

193 **4.2 Precision of the whole system**

194 In order to estimate the precision of the whole system (IC instruments combined with
195 the sampling device including the primary circuit, the pump and the filtration units), we
196 performed a “closed loop” experiment over the course of one day by connecting the
197 inlet and the outlet of the primary circuit to a 300-L tank containing river water. The test
198 was performed three times over two different seasons (the 20th of July 2015, the 28th of
199 August 2015, and the 17th of April 2016). The conductivity probe (one measurement
200 every minute) was used to check the stability of the water chemistry during the course
201 of the experiment (Fig. SI 2). Our results show that a lapse of 2 hours at least is



202 necessary for the system to stabilize, corresponding to the homogenization time of the
 203 water within the closed loop (Fig. 2). After two hours, major anion and cation
 204 concentrations show a remarkable stability indicating the absence of drift over of 24-
 205 hour time lapse despite the temperature variations in the river water, and allowing us to
 206 estimate the precision of the whole system over one day using the standard deviation of
 207 the measurements performed during the test. The results of the test are presented in
 208 Table 2. The precision reached is lower than 0.5% for all species except for potassium,
 209 for which it is lower than 1.2%.

210

211 **4.3 Cross contamination**

212 The ability of the RL to detect rapid variations in river chemistry (typically expected
 213 during storm events) depends on 1) the response time of the RL to a perturbation in the
 214 river and 2) the potential cross contamination from one sample to the next one. We
 215 assessed these two effects by a tracer injection experiment. After establishing a closed
 216 loop experiment (on the 29th of August 2015) and allowing for the period of
 217 stabilization, we introduced a known amount of NaCl (200 g previously dissolved in a
 218 small amount of river water) into the 300-L tank of river water in order to simulate a
 219 “spike” in the river chemistry. The monitoring of conductivity in the primary circuit
 220 allowed us to follow the propagation of the spike injection into the primary circuit while
 221 Cl⁻ concentrations measured by the IC every 40 minutes allowed us to follow its
 222 propagation through the filtration devices and IC instruments (Fig. 3). The conductivity
 223 probe shows that the salinity spike is detected very quickly and stabilized after 5
 224 minutes. This indicates that the water in the primary circuit is quickly homogenized (in
 225 agreement with the high flow rate of the primary circuit: 700 l/h). Conversely, the Cl⁻
 226 and Na⁺ concentrations only reach the expected concentration at the second IC



227 measurement i.e. after 80 minutes.

228

229 The first IC measurement following the spike injection indicates that only 93% of the
 230 final steady-state concentration is reached, revealing a contamination of the (n)th sample
 231 by 7% of the (n-1)th sample. In practice, such a contamination will only be significant if
 232 the instantaneous derivative of river concentration with time is important. In the case of
 233 the Orgeval River, where the RL is deployed, the derivative of the concentration with
 234 respect to time is lower than 1% per hour for 90% of the time for all species. In the case,
 235 identified cross contamination induces an error of 0.07% compared to the true
 236 concentration, which means that the effect of cross contamination is negligible
 237 compared to the precision of the RL (see section 4.2). However, in the case of flood
 238 events, when the stream flow increases quickly, the derivative of concentration can
 239 change by more than 10% per hour. In such cases, cross contamination will induce an
 240 error of 1% or more. The injection test shows that the time resolution of the RL is
 241 limited by the transfer time of the water between sampling and injection into the IC
 242 instruments. This transfer time of the water in the RL is mainly due to the design of the
 243 filtration system, which may be improved in the future.

244

245 **4.4 Reproducibility: RL vs Laboratory**

246 As a final test for assessing the ability of the RL to record fine natural variations of river
 247 chemistry in comparison to conventional techniques of filtration and analyses in the
 248 laboratory, we focused on two days in the summer of 2015 following long periods
 249 without rain (21st of July 2015 for cations and 19th of April 2016 for anions) which
 250 showed very high resolution diurnal variations (<5% relative) in chemical composition
 251 of the Orgeval river. In addition to the analyses made by the RL every 40 minutes, we



252 conducted hourly sampling of the river by collecting 5 litres of water and filtering it
253 immediately using a Teflon[®] frontal filtration unit (Sartorius[®]) with 0.2 μ m
254 polysulfonether filters. Bottles of acidified (at pH = 2) and unacidified river water were
255 transported to the laboratory at IPGP for measurement of major cations and anions,
256 respectively, using IC devices similar to those installed in the RL and calibrated using
257 the same calibration procedure. The error measurement reached in the laboratory is
258 calculated at 1%, estimated through repeated injections of the standard solution “River
259 x1” (every 5 samples). Comparison between the RL and the laboratory for the seven
260 measured species are shown in Figure 4. First, the measurements made by the RL are
261 more precise than those performed in the laboratory, a feature that can be primarily
262 attributed to the greater stability of the continuously working injection system of the
263 RL. Second, the fine variations measured by the RL are reproduced in the laboratory,
264 validating the observed diurnal variations and supporting the reliability of the RL to
265 detect changes on the order of a percent within a day. The third observation is that small
266 yet systematic offsets between the two sets of data exist, up to 3% for Mg. One possible
267 explanation for this difference is that the filtration procedures differed between the RL
268 and the manual sampling, which may have led to a discrepancy in the concentration
269 measurements related to the behaviour of the colloidal phase (Dupré et al., 1999).
270 Regardless of this yet-unexplained discrepancy, we note that variations in concentration
271 recorded by the RL and measured at the IPGP laboratory have the same amplitudes and
272 are synchronous.

273

274 **5 Discussion**

275 **5.1 What are the benefits of bringing the lab into the field?**

276 The RL presented above is a technological breakthrough allowing us to record



continuously, at a high frequency and over long spans of time, the concentration of 7
major dissolved species in a river system. From a scientific point of view - beyond the
scope of the present paper - the RL presented here opens new possibilities for the
exploration of the fine structure of hydrochemical evolution at the catchment scale and
for improved understanding of the associated hydrological, geochemical, and biological
processes. From a technical point of view, our study shows that deploying the
conventional laboratory measurement techniques in the field adds significant value. The
tests performed and reported above clearly demonstrate an improvement in precision
compared to the analysis of bottled samples taken back to the lab. We see three main
reasons for this improvement.

1) In a given river, dissolved concentrations typically vary by less than one order of
magnitude when water discharge changes by several orders of magnitude (Godsey et al.,
2009). This constancy allows us to select a relatively narrow range of concentration for
establishing specific calibration curves of the IC instruments, a condition which is rarely
possible in the laboratory where different kinds of samples are analyzed.

2) While in the laboratory samples are injected discreetly, in the RL river water samples
are injected as a continuous flow. Thus, the primary circuit and the filtration system
operate continuously at a constant pressure, which supports stable and accurate
analyses.

3) The third factor is the experimental conditions in the bungalow. The temperature is
maintained at $24^{\circ}\text{C} \pm 2^{\circ}$ (in addition to the 40°C thermostatically-controlled
temperature in the column, precolumn and detection device of the ICs) allowing for
better stability of the IC measurements. Moreover, the IC instrument is never stopped,
which favours stability.

301



302 **5.2 What is revealed by a higher sampling frequency?**

303 To our knowledge, the high frequency of measurements (one measurement every 40
304 minutes, 0.42 mHz) demonstrated above for the RL installed on the Orgeval River is the
305 highest ever reported for stream chemistry over several months. To highlight the
306 corresponding improvement in the recorded concentration signal, we tested the effect of
307 sampling frequency on the concentration signal. First, we artificially sub-sampled the
308 RL original signal at two lower sampling frequencies: 0.04 mHz (every 7 hours, starting
309 October 5th, 2015 at 10 pm) and 0.01 mHz (every 24 h). The 0.04-mHz frequency was
310 chosen to reproduce the sampling frequency of Neal et al., (2012) made in the
311 Plynlimon watershed, Wales. The 0.01-mHz frequency is typically what is achievable
312 by "human grab-sampling" in the field. Second, we calculated the probability density
313 function (PDF) of concentration measurements over a given time interval.

314 The use of PDFs allows us to explore the structure of concentration signals beyond the
315 mean concentration, which constitutes an important metric for river solute budget, but
316 lacks any insight into the variations in concentrations that can be used to retrieve
317 information on catchment processes. A PDF can be described by 4 statistical parameters
318 (mean, standard deviation, skewness, and kurtosis) that account, at first-order, for the
319 fine structure of a concentration signal. We compared these four parameters for the
320 computed PDFs to quantify the signal degradation induced by artificial sub-sampling.
321 Skewness indicates the distribution asymmetry, both in magnitude and direction
322 (positive skewness means that most values are higher than the mean), while Kurtosis is
323 a measure of the "tailedness" of the distribution. For a given distribution (*i.e.* a given
324 standard deviation and skewness), a lower kurtosis indicates fewer extreme outliers.

325 We applied this statistical approach to two representative periods of the hydrological
326 cycle of the Orgeval Critical Zone Observatory: a typical 6-day flood event caused by



the arrival of a wet, Atlantic meteorological front (in October 2015) and a dry summer low water stage period (July 2015) where the stream is essentially sustained by groundwater (an apparently “boring” hydrological period). We first presented the behaviour of calcium and sulphate concentrations as an example during the two considered periods (Fig. 5 and 6), before generalizing to all measured species (Fig. 7).

332

Flood event. The Ca concentration time series recorded at 0.42 mHz (every 40-minutes) shows that minimum Ca concentrations are recorded at maximum water discharge, but this relationship is invisible at lower sampling frequency (Fig. 5). Narrow peaks during the maximum of the stream flow are unresolved at a daily or 7-hourly frequency. The comparison of the calculated PDF shows that a bimodal character is captured at all frequencies. The average and standard deviation are not significantly affected by the sampling frequency, with a relative difference of less than 2% for the values of these parameters between the three distributions. However, the skewness and kurtosis values vary among the different records. From the 0.42 mHz to 0.01 mHz signals, skewness values decrease by about 50%, which means that even if the overall concentration variability is well captured at the lower sampling frequencies, the concentration signal is clearly degraded. This degradation is particularly intense during the maximum flood event, where the concentration signal evolves quickly.

346

Summer event. Despite the absence of rain events during the 2015 summer, the River Lab recorded high frequency variations revealing a diurnal structure with 7% relative variations between day and night and specific to each element. The figure 6 shows that the structure of this signal is altered when the sampling frequency decreases. While these daily variations are still captured when sampling occurs every 7 hours, their



352 amplitude is somewhat altered (5%) compared to the 0.42 Hz sampling frequency (8%).
353 The daily structure of the signal is absent on the 0.01 mHz sampling frequency. While
354 the mean remains the same over the range of sampling frequency, the variability
355 quantified by the relative standard deviation decreases with lower sampling frequency,
356 by up to 50% for the daily frequency compared to the 0.42 mHz signal, indicating a
357 significant loss of information. The skewness of the concentration distribution recorded
358 at a sub-sampled daily frequency has a value that is opposite in sign compared to the
359 other two frequencies, indicating that there is an inversion of the measured asymmetry
360 of the PDF at lower sampling frequencies. Therefore, too coarse of a sampling
361 frequency can yield a strongly altered signal compared to higher frequencies, resulting
362 in a biased shape of the distribution of the concentrations.

363

364 **Generalization.** The resampling approach applied above can be generalized and
365 expanded to other elements for both the summer and flood events. In figures 5 and 6,
366 we arbitrarily chose the hour of sampling (10 a.m. and 2p.m. for Figures 5 and 6,
367 respectively). In figure 7, the sub-sampling is performed at each of the possible
368 sampling hours: 24 for the 0.01 mHz sampling frequency (one time a day) and at each
369 of the 7 for the 0.04 mHz sampling frequency (every 7 hours). For each of these
370 sampling hours we computed the PDF of every element concentration and presented the
371 average and the standard deviation (Fig. 7) of the four statistical parameters already
372 discussed above.

373 Figure 7 shows that the concentration PDF are strongly sensitive to the sampling
374 frequency. The standard deviation, reflecting variability of the concentration,
375 systematically decreases with the sampling frequency indicating narrower distributions
376 at low frequencies. This consequence of sampling frequency on signal variability is



377 more important during the summer event compared to the flood event, where the
378 amplitude of flood event concentration variations are much higher (30-40%) compared
379 to the summer event (8%). Skewness and kurtosis are clearly the most affected
380 parameters when the sampling frequency is decreased. Depending on the element,
381 skewness varies as a function of sampling frequency, from +100% to -300% for the
382 summer event and from +50% to -100% for the flood event, indicating complete
383 changes in the asymmetry of the PDFs. Changes in the kurtosis are even more
384 pronounced between 0.42 and 0.01mHz, ranging from +1000% to -2600% in summer
385 and 0 to 700% for the flood event. This statistical analysis quantitatively demonstrates
386 that only high frequency measurements are able to capture the day-night chemical
387 cycles of the Orgeval River. Given the amplitude and duration of typical flood events in
388 the catchment, the alteration of the signal by lowering the sampling frequency is less
389 critical but still significant during these periods.

390

391 **5.3 What is revealed by better analytical precision?**

392 As shown above, the Orgeval RL not only achieves high frequency measurements but
393 also produces improved precision compared to conventional lab analysis following
394 manual sampling. Therefore, any sampling procedure, even at a high frequency,
395 involving conventional lab analysis induces a loss of precision. We demonstrate this
396 effect through a numerically generated artificial degradation of the precision. Using the
397 original RL concentration signal as a reference, we artificially degraded the signals by
398 adding a normally distributed noise onto the concentration signals recorded by the RL.
399 Noise levels of 4% and 2% were tested; as they are representative of the relative
400 analytical precision reported for most laboratory IC devices (Neal et al. 2011; Aubert et



401 al., 2013a). The same representative periods as in the previous section (summer and
402 flood events) were utilized for these tests.

403

404 **Flood event.** The figure 8 illustrates the concentration PDF obtained after degradation
405 of the analytical precision for the Ca concentration. The narrow peaks recorded during
406 the maximum of the stream flow are virtually invisible in the signal at a 4%-precision,
407 and strongly smoothed in the signal at a 2%-precision. The original bimodal
408 characteristic of the PDF is still visible in the 2%-precision signal but no longer in the
409 4%-precision signal. The mean and standard deviation appear to be insensitive to these
410 changes in analytical precision, while skewness and kurtosis are strongly impacted,
411 reflecting significant alteration of the concentration PDF at lower precision.

412

413 **Summer event.** Figure 9 shows how the sulphate concentration signal is affected when
414 the precision is degraded. Day-night variations are only visible in the original RL signal
415 because of its high analytical precision. The effect of degraded precision on the PDFs is
416 more important than for the flood event (Fig. 8). While the mean value is robust, the
417 standard deviation is altered (+150% from the RL signal to the 4% precision signal).
418 The skewness decreases by up to 90% for the signal at 4%-precision compared to the
419 original signal and 74% for the signal at 2%-precision, indicating that the original RL
420 signal asymmetry is lost as precision is compromised. These changes in the parameters
421 of the concentration PDF show that the structure of the concentration signal in the
422 Orgeval River would be significantly altered if the measurements were made with
423 analytical precision lower than that of the RL prototype.

424



425 **Generalization.** This approach has been expanded to other elements for both the
426 summer and flood events, as shown in the figure 10, indicating that concentration PDFs
427 are strongly sensitive to the analytical precision for all species. For both selected events
428 (flood and drought), changes in the four statistical parameters are more significant for
429 the 4% precision signal than for the 2% precision signal. The average is not sensitive to
430 analytical precision. The standard deviation systematically increases as the precision is
431 compromised, leading to a much larger variability at low precision. Skewness and
432 kurtosis decrease for all elements considered both for the flood and drought event.
433 Given that the concentration PDF calculated from the RL original signal is
434 asymmetrical with a positive skewness, this observation indicates that the PDFs become
435 more symmetrical and flatten at degraded analytical precision.
436 Based on the resampling test, the observed effects are more drastic for the summer
437 event than for the flood event, indicating that the high precision record is particularly
438 necessary in order to capture subtle day-night variations.

439

440 **6 Conclusion**

441 This paper demonstrates the feasibility of deploying conventional laboratory
442 instruments in the field to measure the concentration of major dissolved anions and
443 cations in rivers (Na^+ , K^+ , Mg^{2+} , Ca^{2+} , Cl^- , SO_4^{2-} , NO_3^-) at a high frequency (0.42 mHz,
444 i.e. one measurement every 40 minutes) and at a high analytical precision (better than
445 1%) over several months. The RL prototype was installed in the Avenelles stream at the
446 Orgeval Critical Zone Observatory, France. The RL features physico-chemical probes,
447 an on-line 0.2- μm -filtration system, and two ionic chromatographic devices, all
448 installed in a closed, air-conditioned bungalow. The RL is autonomous, operable at
449 distance and data can be transmitted automatically. Human intervention is required only



450 once a week. Therefore, the RL also allows for an efficient attribution of human
451 resources, as well as considerable saving of consumables.

452 A suite of tests performed on the RL to assess quality measurement and to compare
453 with more conventional "grab sampling" followed by laboratory measurements revealed
454 only a minor drift in the instrument calibration, leading to improved precision. This
455 precision is not easily achieved in the laboratory under standard analysis conditions,
456 showing the benefit of transporting the laboratory devices to the field. The analytical
457 breakthrough made possible by the RL for major dissolved elements could theoretically
458 be extended to other elements separable by ion chromatography. Preliminary tests
459 demonstrate that species present in trace amounts in river water (down to the ppb, such
460 as strontium or lithium) could be measured with the same gain in precision.

461 For this particular prototype, the measurement frequency (0.42 mHz) appears to be
462 limited by the turnover time of water in the filtered water circuit, which is in turn
463 imposed by the filtration unit. However, the high frequency and high precision of the
464 RL enabled unprecedented observations of the fine structure in hydrochemical time
465 series. Their interpretation is beyond the scope of the present proof-of-concept paper but
466 the RL is able to capture the abrupt changes in dissolved species concentrations during a
467 typical 6-days flood event, as well as unexpected daily oscillations during a
468 hydrological 'boring' period of summer drought.

469 Using the high frequency signal as a benchmark, it is possible to artificially alter the
470 sample frequency and the analytical precision and study the resulting effect on the
471 geochemical distribution obtained for characteristic hydrological events. This analysis
472 shows that in order to retrieve the fine structure of the hydrochemical signal, high
473 sampling frequency and improved analytical precision are both necessary conditions. To
474 paraphrase Jim Kirchner's quote: "If we want to understand the full symphony of



475 catchment hydrochemical behaviour, then we need to be able to hear every note". The
476 improvements made possible by the RL make it, to date, the best orchestra available to
477 play the potamological symphony.

478 Our study opens a new era of investigation into the fine structure of the hydrochemical
479 signal in rivers. Future work will explore the relationships between the desired
480 measurement frequency and the timescales of the complex interactions between primary
481 and secondary minerals, biotic processes and hydrological processes that are taking
482 place in catchment systems. Recording such fine stream hydrochemical variations is
483 thus offering a new perspective on Critical Zone.

484

485 **Author's information**

486 Corresponding author: *E-mail: floury@ipgp.fr and gaillardet@ipgp.fr

487

488 **Acknowledgment**

489 This work was supported by the EQUIPEX CRITEX programme, (grant # ANR-11-
490 EQPX-0011) and funding from IRSTEA (Institut national de recherche en
491 sciences et technologies pour l'environnement et l'agriculture).

492 We would like to thanks, D. Calmels, P. Louvat, J. Kirschner, J. Druhan, S. Brantley, B.
493 McDowell and J. Chorover for helpful comments. S. Losa (Thermo Fisher), C. Fagot, P.
494 Reignier and M. Bauer from Endress+Hauser Company are thanked for technical
495 assistance. PF benefited from a doctorate grant from MESR, France. The Orgeval CZO
496 river basin belongs to the French National Infrastructure OZCAR (Observatoires de la
497 Zone Critique).

498

499

500



References

- a) Aubert, A. H., Gascuel-Oudou, C., Gruau, G., Akkal, N. et al. Solute transport dynamics in small, shallow groundwater-dominated agricultural catchments: insights from a high-frequency, multisolute 10 yr-long monitoring study. *Hydrol. Earth Syst. Sci.* 2013, 17, 1379–1391.
- b) Aubert, A. H., Gascuel-Oudou, C., Merot P. Annual hysteresis of water quality: A method to analyse the effect of intra- and inter-annual climatic conditions. *Journal of Hydrology*. 2013, 478, 29–39.
- Aubert, A.H., Kirchner, J. W., Gascuel-Oudou, C., Faucheux, M. et al. Fractal Water Quality Fluctuations Spanning the Periodic Table in an Intensively Farmed Watershed. *Environ. Sci. Technol.* 2014, 48, 930–937.
- Azzaro F., Galletta M. Automatic colorimetric analyzer prototype for high frequency measurement of nutrients in seawater. *Marine Chemistry*. 2006, 99, 191–198.
- Bain R., Gundry S., Wright J., Yang H., Pedley S., Bartram J. Accounting for water quality in monitoring access to safe drinking-water as part of the Millennium Development Goals: lessons from five countries. *Bull World Health Organ.* 2012, 90, 228–235.
- Banna M., Imran S., Francisque A., Najjaran H., Sadiq R., Rodriguez M., Hoorfar M. Online Drinking Water Quality Monitoring: Review on Available and Emerging Technologies. *Environ. Sci. Technol.* 2014, 44, 1370–1421.
- Bartram J., Ballance R. Water Quality Monitoring. A practical guide to the design and implementation of freshwater quality studies and monitoring programmes. *United Nations Environment Programme*. 1996, 400 pages.
- Beck A. J., Janssen F., Polerecky L., Herlory O., De Beer D. Phototrophic Biofilm Activity and Dynamics of Diurnal Cd Cycling in a Freshwater Stream. *Environ. Sci. Technol.* 2009, 43, 7245–7251.
- Brick, CM., Moore J. N. Diel variation of trace metals in the upper Clark Fork River, Montana. *Environ Sci Technol.* 1996, 30, 1953–1960.
- Calmels D., Galy A., Hovius N., Bickle M., West A., Chen M., Chapman H. Contribution of deep groundwater to the weathering budget in a rapidly eroding mountain belt, Taiwan. *Earth and Planetary Science Letters*. 2011, 303 48–58.
- Cassidy R., Jordan P. Limitations of instantaneous water quality sampling in surface-water catchments: Comparison with near-continuous phosphorus time-series data. *Journal of Hydrology*, 2011, 405, 182–193.
- Chan E., Kessler J., Shiller A., Joung D., Colombo F. Aqueous Mesocosm Techniques Enabling the Real-Time Measurement of the Chemical and Isotopic Kinetics of Dissolved Methane and Carbon Dioxide. *Environ. Sci. Technol.* 2016, 50, 3039–3046.



- 550
551 Chapman D. Water Quality Assessments - A Guide to Use of Biota, Sediments and
552 Water in Environmental Monitoring - Second Edition. *United Nations Environment*
553 *Programme*, 1996, 651 pages.
554
555 Chapman, P. J., Reynolds, B., Wheeler, H. S. Sources and controls of calcium and
556 magnesium in storm runoff: the role of groundwater and ion exchange reactions along
557 water flowpaths. *Hydrol Earth Syst Sci.* 1997, 1, 671–685.
558 283, 3–17.
559
560 Clough T., Buckthought L., Kelliher F., Sherlock R. Diurnal fluctuations of dissolved
561 nitrous oxide (N₂O) concentrations and estimates of N₂O emissions from a spring-fed
562 river: implications for IPCC methodology. *Global Change Biology*. 2007. 13, 1016–
563 1027.
564
565 Dåbakk E., Nilsson M., Geladi P., Wold S., Renberg I. Sampling reproducibility and
566 error estimation in near infrared calibration of lake sediments for water quality
567 monitoring. *Journal of Near Infrared Spectroscopy*, 1999, 7, 241–250.
568
569 Danielsen F., Burgess N. et al. Local Participation in Natural Resource Monitoring: a
570 Characterization of Approaches. *Conservation Biology*, 2008, 23, 31–42.
571
572 de Montety, V., Martin, J.B., Cohen, M.J., Foster, C., Kurz, M.J., Influence of diel
573 biogeochemical cycles on carbonate equilibrium in a karst river. *Chemical Geology*.
574 2011, 283, 31–43.
575
576 Dupré B., Viers J., Dandurand J.L., Polve M., Bénézech P., Vervier P., Braun J.J.. Major
577 and trace elements associated with colloids in organic-rich river waters: ultrafiltration of
578 natural and spiked solutions. *Chemical Geology*, 1999, 160, 63–80.
579
580 Feng, X. H., Kirchner, J. W., Neal, C. Measuring catchment-scale chemical retardation
581 using spectral analysis of reactive and passive chemical tracer time series. *Journal of*
582 *Hydrology*. 2004, 292, 296–307.
583
584 Gammons, C. H., Grant T. M., Nimick, D. A., Parker, S. R., DeGrandpre, M. D. Diel
585 changes in water chemistry in an arsenic-rich stream and treatment-pond system.
586 *Science of the Total Environment*. 2007, 384, 433–451.
587
588 Garnier J., Billen, G., Vilain, G., Benoit, M., Passy, P., Tallec, G., Tournebize, J., et al.
589 Curative vs. preventive management of nitrogen transfers in rural areas: Lessons from
590 the case of the Orgeval watershed (Seine River basin, France). *Journal of*
591 *Environmental Management*. 2014, 144, 125–134.
592
593 Glasgow H., Burkholder J., Reed R., Lewitus A., Kleinman J. Real-time remote
594 monitoring of water quality: a review of current applications, and advancements in
595 sensor, telemetry, and computing technologies. *Journal of Experimental Marine*
596 *Biology and Ecology*, 2004, 300, 409–448.
597
598 Halliday S., Skeffington R., Wade A., Bowes M., Gozzard E., Newman J., Loewenthal
599 M., Palmer-Felgate E., Jarvie H. High-frequency water quality monitoring in an urban



- 600 catchment: hydrochemical dynamics, primary production and implications for the Water
601 Framework Directive. *Hydrological Processes*. 2015, 29, 3388–3407.
- 602
- 603 Huang K., Cassar N., Jonsson B., Cai W., Bender M. An Ultrahigh Precision, High-
604 Frequency Dissolved Inorganic Carbon Analyzer Based on Dual Isotope Dilution and
605 Cavity Ring-Down Spectroscopy. *Environ. Sci. Technol.* 2015, 49, 8602–8610.
- 606
- 607 Jasechko, S., Kirchner, J. W., Welker, J. M., McDonnell, J. J. Substantial proportion of
608 global streamflow less than three months old. *Nature Geoscience*. 2016, 9, 126–130.
- 609
- 610 JCGM 200:2012. International vocabulary of metrology – Basic and general concepts
611 and associated terms (VIM). 2012.
- 612
- 613 Jones T., Chappell N., Tych W. First Dynamic Model of Dissolved Organic Carbon
614 Derived Directly from High-Frequency Observations through Contiguous Storms.
615 *Environ. Sci. Technol.* 2014, 48, 13289–13297.
- 616
- 617 Jordan P., Cassidy R. Technical Note: Assessing a 24/7 solution for monitoring water
618 quality loads in small river catchments. *Hydrol. Earth Syst. Sci.*, 2011, 15, 3093–3100.
- 619
- 620
- 621
- 622 Kirchner, J. W., Feng, X., Neal, C. Fractal stream chemistry and its implications for
623 contaminant transport in catchments. *Nature* 2000, 403, 524–527.
- 624
- 625 Kirchner, J. W., Feng, X., Neal, C. Catchment-scale advection and dispersion as a
626 mechanism for fractal scaling in stream tracer concentrations. *J Hydrol.* 2001, 254, 81-
627 100.
- 628
- 629 Kirchner, J. W., Feng, X., Neal, C., Robson, A. J. The fine structure of water-quality
630 dynamics: the (high-frequency) wave of the future. *Hydrological Processes*. 2004, 18,
631 1353–1359.
- 632
- 633 Kirchner, J. W. Getting the right answers for the right reasons: Linking measurements,
634 analyses, and models to advance the science of hydrology. *Water Resour. Res.* 2006, 42,
635 1–5.
- 636
- 637 Kurz, M. J., de Montety, V., Martin, J. B., Cohen, M. J., Foster, C. R. Controls on diel
638 metal cycles in a biologically productive carbonate-dominated river. *Chemical Geology*.
639 2013, 358, 61–74.
- 640
- 641 Liu, Z., Liu, X., Liao, C., Daytime deposition and nighttime dissolution of calcium
642 carbonate controlled by submerged plants in a karst spring-fed pool: insights from high
643 time-resolution monitoring of physico-chemistry of water. *Environ Geol.* 2008, 55,
644 1159–1168.
- 645
- 646 Macintosh K., Jordan P., Cassidy R., Arnscheidt J., Ward C. Low flow water quality in
647 rivers, septic tank systems and high-resolution phosphorus signals. *Science of the Total*
648 *Environment*, 2011, 412, 58–65.
- 649



- 650 Morel, B., Durand, P., Jaffrezic, A., Gruau, G., Molenat, J. Sources of dissolved
651 organic carbon during storm flow in a head-water agricultural catchment, *Hydrological*
652 *Processes*. 2009, 23, 2888–2901.
- 653
- 654 Neal, C., Watts, C., Williams, R. J., Neal, M., Hill, L., Wickham, H. Diurnal and longer
655 term patterns in carbon dioxide and calcite saturation for the River Kennet, south-
656 eastern England. *The Science of the Total Environment*. 2002, 205–231.
- 657
- 658 Neal, C., Reynolds, B., Norris, D., Kirchner, J. W., Neal, M., Rowland, P., et al. Three
659 decades of water quality measurements from the Upper Severn experimental catchments
660 at Plynlimon, Wales: an openly accessible data resource for research, modelling,
661 environmental management and education. *Hydrological Processes*. 2011. 25, 3818–
662 3830.
- 663
- 664 Neal, C., Reynolds, B., Rowland, P., Norris, D., Kirchner, J. W., Neal, M., Sleep, D.,
665 Lawlor, A., Woods, C., Thacker, S., Guyatt, H., Vincent, C., Hockenhull, K., Wickham,
666 H., Harman, S., Armstrong, L. High-frequency water quality time series in precipitation
667 and streamflow: From fragmentary signals to scientific challenge. *Sci. Total Environ.*
668 2012, 434, 3–12.
- 669
- 670 Nimick, D. A., Cleasby, T. E., McCleskey, R. B. Seasonality of diel cycles of dissolved
671 trace metal concentrations in a Rocky Mountain stream. *Environ Geol.* 2005, 47, 603–
672 614.
- 673
- 674 Nimick, D. A., Gammons, C. H., Parker, S. R. Diel biogeochemical processes and their
675 effect on the aqueous chemistry of streams: A review. *Chemical Geology*. 2011,
676
- 677 a) Rozemeijer J., Klein J., Broers H., van Tol-Leenders T., van der Grift B. Water
678 quality status and trends in agriculture-dominated headwaters, a national monitoring
679 network for assessing the effectiveness of national and European manure legislation in
680 The Netherlands. *Environ Monit Assess*, 2014, 186, 8981–8995.
- 681
- 682 b) Rozemeijer J., van der Velde Y., van Geer F., Bierkens M., Broers H. Direct
683 measurements of the tile drain and groundwater flow route contributions to surface
684 water contamination: From field-scale concentration patterns
685 in groundwater to catchment-scale surface water quality. *Environmental Pollution*,
686 2010, 158, 3571–3579.
- 687
- 688 Rozemeijer J., van der Velde Y., de Jonge H., van Geer F., Broers H., Bierkens M.
689 Application and Evaluation of a New Passive Sampler for Measuring Average Solute
690 Concentrations in a Catchment Scale Water Quality Monitoring Study. *Environ. Sci.*
691 *Technol.* 2010, 44, 1353–1359.
- 692
- 693 Strobl R., Robillard P. Network design for water quality monitoring of surface
694 freshwaters: A review. *Journal of Environmental Management*, 2008, 87, 639–648.
- 695
- 696 Takagi, M. Water chemistry of headwater streams under storm flow conditions in
697 catchments covered by evergreen broadleaved forest and by coniferous plantation
698 Landscape Ecol Eng. 2015, 11, 293–302.
- 699



- 700 Telci I., Nam K., Guan J., Aral M. Optimal water quality monitoring network design for
701 river systems. *Journal of Environmental Management*, 2009, 90, 2987–2998.
- 702
- 703 Tercier-Waeber M., Hezard T., Masson M., Schäfer J. In Situ Monitoring of the Diurnal
704 Cycling of Dynamic Metal Species in a Stream under Contrasting Photobenthic Biofilm
705 Activity and Hydrological Conditions. *Environ. Sci. Technol.* 2009, 43, 7237–7244.
- 706
- 707 Vuillemin R., Le Roux D., Dorval P., Bucas K., Sudreau J. P., Hamon M., Le Gall C.,
708 Sarradin P. M. CHEMINI: A new in situ CHEmical MINiaturized analyzer. *Deep-Sea*
709 *Research I.* 2009, 56, 1391–1399.
- 710
- 711 von Freyberg, J., Studer, B., and Kirchner, J. W.: A lab in the field: high-frequency
712 analysis of water quality and stable isotopes in streamwater and precipitation, *Hydrol.*
713 *Earth Syst. Sci. Discuss.*, doi:10.5194/hess-2016-585, in review, 2016.
- 714
- 715
- 716 Wang Z., Sonnichsen F., Bradley A., Hoering K., Lanagan T., Chu S., Hammar T.,
717 Camilli R. In Situ Sensor Technology for Simultaneous Spectrophotometric
718 Measurements of Seawater Total Dissolved Inorganic Carbon and pH. *Environ. Sci.*
719 *Technol.* 2015, 49, 4441–4449.
- 720
- 721 Whitehead P., Wilby R., Battarbee R., Kerman M., Wade A. A review of the potential
722 impacts of climate change on surface water quality. *Hydrological Sciences–Journal–des*
723 *Sciences Hydrologiques*, 2009, 54, 101–121.
- 724
- 725 Yang W., Nan J., Sun D. An online water quality monitoring and management system
726 developed for the Liming River basin in Daqing, China. *Journal of Environmental*
727 *Management*, 2008, 88, 318–325.
- 728
- 729 Zabiegała B., Kot-Wasik A., Urbanowicz M., Namieśnik J. Passive sampling as a tool
730 for obtaining reliable analytical information in environmental quality monitoring. *Anal*
731 *Bioanal Chem*, 2010, 396, 273–296.
- 732 Kunz A., Steinmetz R., Damasceno S., Coldebela A. Nitrogen removal from swine
733 wastewater by combining treated effluent with raw manure. *Sci. Agric.*, 2012, 69, 352–
734 356.
- 735
- 736 Zhu X., Li D., He D., Wang J., Ma D., Li F. A remote wireless system for water quality
737 online monitoring in intensive fish culture. *Computers and Electronics in Agriculture*,
738 2010, 71, 3–9.
- 739
- 740
- 741
- 742
- 743
- 744
- 745
- 746
- 747



748 **Table**

749 **Table 1. Assessment of the RL accuracy and instrumental drift based on concentration**
 750 **measurements made after several injections of the standard solution "River x1". The uncertainty**
 751 **on the calibration solution is the quadratic sum of the uncertainty on the standard solutions**
 752 **(provided by the manufacturer) and the overall uncertainty for weighing during solution**
 753 **preparation. Measurement errors over one week and over two months are expressed as the relative**
 754 **standard deviation (RSD) calculated based on the injections of the solution "River x1" directly into**
 755 **the IC instruments via the multiport valve (see Fig. 1).**

756
 757
 758 **Table 2. Precision on concentration measurements of the whole RL system**
 759 **calculated as the relative standard deviation (RSD) of concentration measurements**
 760 **made over three 24-hour closed loop experiments, during which the inlet and the**
 761 **outlet of the primary circuit are connected through a 300-L tank of river water.**

762
 763
 764
 765
 766
 767
 768
 769
 770
 771
 772
 773
 774
 775
 776
 777
 778
 779
 780
 781
 782
 783
 784
 785
 786
 787
 788
 789
 790
 791
 792
 793
 794
 795
 796
 797



Figure Captions

Figure 1. Sketch of the River Lab. Bold blue arrows indicate the primary circuit of unfiltered water. Dashed arrows indicate filtered water supplied to IC instruments. 1: The inlet of the primary circuit samples the river at a constant 20-cm depth maintained by buoys. Water is filtered at < 2 mm using a strainer. The distance between the mouth and the pump is 6 m. The primary circuit assembly is almost entirely composed of polyvinyl chloride (PVC) pipes. 2: The electric pump runs continuously at a constant power, leading to a rate of 700 liters per hour. 3: Almost all the river water just flows through the pipe and remains unfiltered. A fraction is filtered at < 2 μm through a tangential stainless steel filtration unit, then filtered through a cellulose acetate frontal filter at < 0.2 μm and finally delivered to IC instruments at a flow rate of 1 liter per hour. 4: A multiport valve before introduction to the IC instruments allows for switching between filtered river water and standard or blank solutions. 5: All probes are deployed in an overflow tank of 5 liters of unfiltered river water. 6: The outlet of the primary circuit is downstream in the river.

Figure 2. Assessment of the precision of the whole RL system including the primary circuit, filtration systems and IC instruments. A closed system is established on the primary circuit of the RL by connecting the inlet and the outlet through a 300-L tank of river water. The system is then run for a period of 24 hours. The figure illustrates the relative variation of concentration (C) of four dissolved species in percentage of relative deviation compared to the mean concentration (C_{mean}). This particular test was performed on the 17th of April 2016. The time between two IC analyses is 40 minutes. The purple curve represents data of temperature of the water in the tank. We do not consider the 2 first hours (3 first measurements), corresponding to the homogenization of water in the circuit and tank (see conductivity measurements in Fig. SI 2) for the calculation of precision.

Figure 3. Assessment of the effects of cross contamination and response time in concentration measurements of the RL system using a tracer (NaCl) injection experiment. A closed system is established on the primary circuit of the RL by connecting the inlet and outlet through a 300-L tank of river water. Then, 200 g of salt previously dissolved in a small amount of river water are injected instantaneously right after one measurement in the closed system to generate a “spike”. The conductivity measurement frequency is 1 per minute, whereas the time between two measurements of chloride concentration is 40 minutes. Error bars for conductivity and Cl⁻ concentration measurements are smaller than their symbols. Results are normalized to the difference between the minimum value, before the tracer injection (0%) and the maximum value, at the end of the experiment (100%).



Figure 4. Assessment of the reproducibility of IC measurements made by the RL every 40 minutes (blue), based on concentration measurements made in the laboratory after conventional sampling every hour (orange), performed the 21st of July 2015 for the cationic species and the 19th of April 2016 for the anionic species. For measurements performed in the laboratory, the error measurement is 1% (except for K⁺ at 2%) calculated as the standard deviation over repeated injection of the standard solutions “River x1”. For RL measurements the error is given in table 2.

Figure 5. Calcium concentration and stream flow in the Orgeval river during a flood event (from the 1st to the 25th of October 2015), sampled every 40 minutes (RL original signal at 0.42 mHz) and artificially sub-sampled every 7 hours (0.04 mHz), and every day (0.01 mHz) at 10 a.m.. Dashed vertical lines indicate the three stream flow peaks. Black dots represent data during the flood event strictly (from the 5th of October 2015 to the 10th of October 2015 at 10 a.m.), over which probability density functions (PDFs) of concentration are calculated and represented as histograms (right panels). For each PDF, the following statistical parameters are calculated: average (Ave.), standard deviation (Std D.), skewness (Skew) and kurtosis (Kur.). Gray dots represent concentration values outside of the flood event and are not considered in the corresponding PDF.

Figure 6. Sulphate concentration in the Orgeval river during a summer event (from the 7th to the 19th of July 2015) sampled every 40 minutes (RL original signal at 0.42 mHz) and artificially sub-sampled every 7 hours (0.04 mHz), and every day (0.01 mHz) at 2 p.m.. Probability density functions (PDF) of concentration are represented as histograms (right panels). For each PDF, the following statistical parameters are calculated: average (Ave.), standard deviation (Std D.), skewness (Skew) and kurtosis (Kur.).

Figure 7. Values of the four statistical parameters obtained from the Orgeval River concentration PDF for the seven dissolved species measured by the RL. From the top to the bottom: average, standard deviation, skewness and kurtosis. The statistical parameters are calculated from data collected over two periods: ‘flood event’ (left panels) and ‘summer event’ (right panels). Each statistical parameter is calculated for three sampling frequencies: every 40 minutes (RL original signal at 0.42 mHz) and artificially sub-sampled every 7 hours (0.04 mHz) and every day (0.01 mHz). For each statistical parameter, the value obtained from the RL original signal is considered the reference against which all values are compared. The figure thus shows the relative deviation of the four statistical parameter values of the sub-sampled signals compared to the RL original signal-derived value, in %. For the daily and 7-hourly frequency signals, the value reported for each statistical parameter is the average over the 24 and 7 possible sub-sampling schemes (one every hour), respectively; and the error bar corresponds to the standard deviation of these statistical parameters over these 24 and 7 possible sub-sampling schemes respectively.



898 **Figure 8. Calcium concentration and stream flow in the Orgeval river during a**
 899 **flood event (from the 1st to the 25th of October 2015), as recorded by RL and for**
 900 **two artificially degraded signals using a normally distributed noise with standard**
 901 **deviation of 2% and 4%, to reflect the effect of decreased analytical precision.**
 902 **Black dots represent data during the flood event strictly from the 5th of October**
 903 **2015 at 12 a.m. through 10th of October 2015). The probability density functions**
 904 **(PDF) of concentration are calculated and represented as histograms (right**
 905 **panels). For each PDF, the following statistical parameters are calculated: average**
 906 **(Ave.), standard deviation (Std D.), skewness (Skew) and kurtosis (Kur.). Gray**
 907 **dots represent concentration values outside of the flood event, which are not**
 908 **considered for the analysis presented on the right panels.**

911 **Figure 9. Sulphate concentration in the Orgeval river recorded by the RL during**
 912 **two weeks in summer (from 7th of July 2015 through 19th of July 2015), and for two**
 913 **artificially degraded signals, using a normally distributed noise with a standard**
 914 **deviation of 2% and 4%, to reflect the effect of degraded analytical precision. The**
 915 **probability density functions (PDF) of concentration are calculated and**
 916 **represented as histograms (right panels). The average (Ave.), standard deviation**
 917 **(Std D.), skewness (Skew) and kurtosis (Kur.) are calculated for each PDF.**

920 **Figure 10. Values of the four statistical parameters obtained from the Orgeval**
 921 **River concentration PDF for the seven dissolved species measured by the RL.**
 922 **From the top to the bottom: average, standard deviation, skewness and kurtosis.**
 923 **The statistical parameters are calculated from data collected over two periods (see**
 924 **text): ‘Flood event’ (left panels) and ‘Summer event’ (right panels). Each statistical**
 925 **parameter is calculated for three different signals: the original RL signal**
 926 **(characterized by an analytical precision over one week, given in Tab. 1) and two**
 927 **artificially degraded signals using a normally distributed noise with standard**
 928 **deviation of 2% and 4%, to reflect the effect of analytical uncertainty. For each**
 929 **event and each level of precision, the concentration PDF were computed 10,000**
 930 **times. For each statistical parameter, the value obtained from the RL original**
 931 **signal was considered as a reference value against which all numerical values are**
 932 **compared. We thus present the relative deviation of the value of the four statistical**
 933 **parameters for the artificially degraded signals compared to the RL original signal-**
 934 **derived value, in %. The value and error bar reported for each statistical**
 935 **parameter is the average and standard deviation over the 10,000 calculations,**
 936 **respectively.**



Figure 1

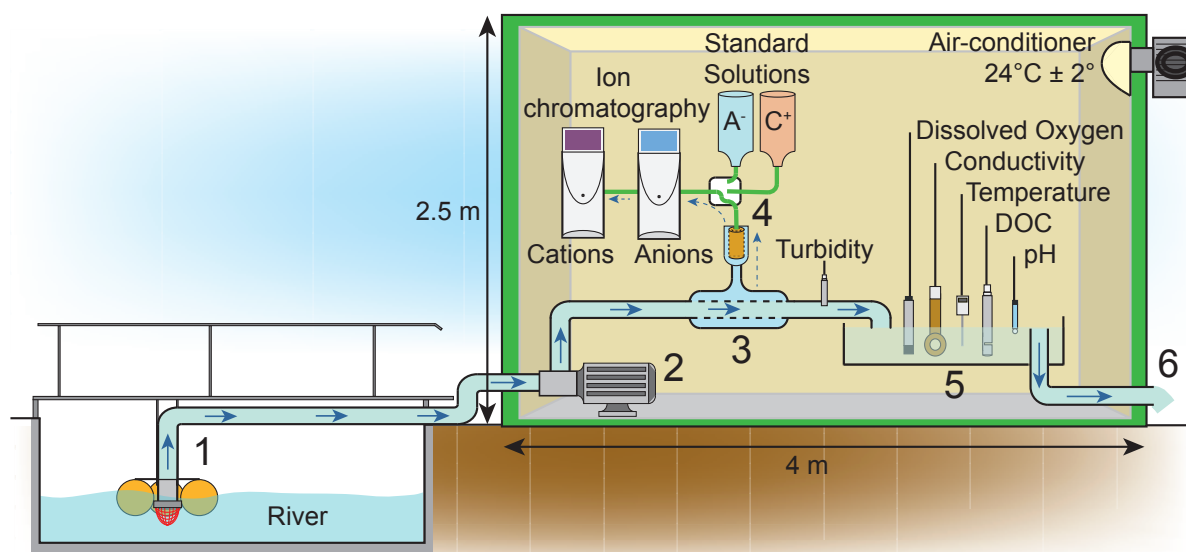




Figure 2

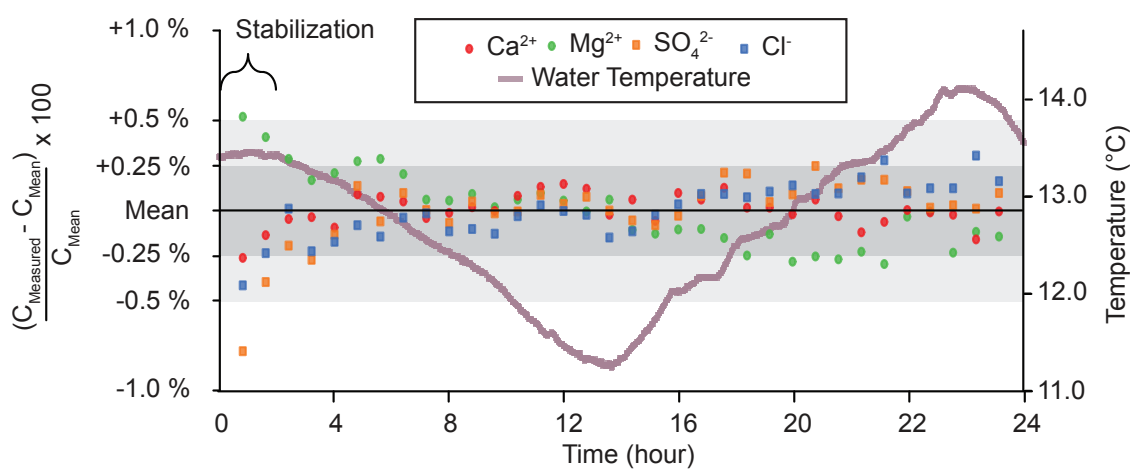




Figure 3

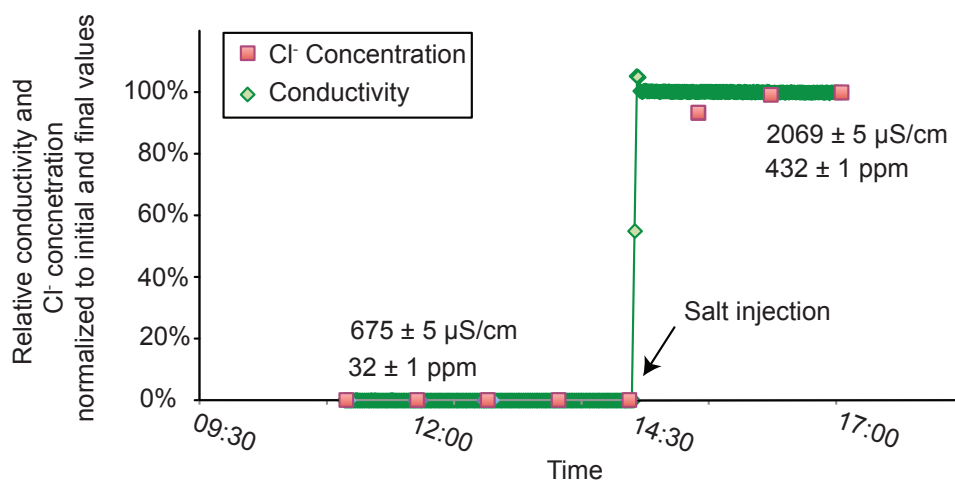




Figure 4

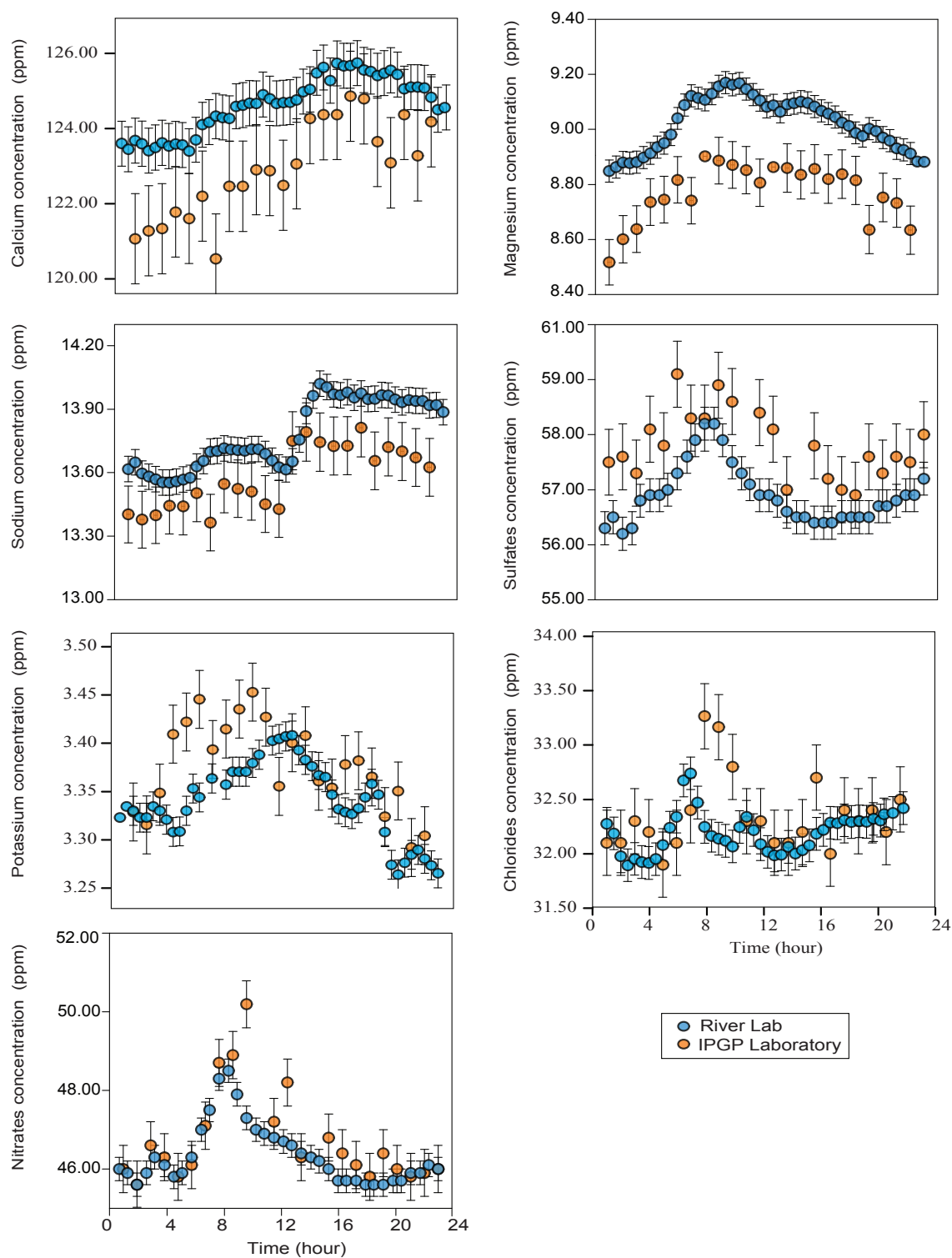




Figure 5

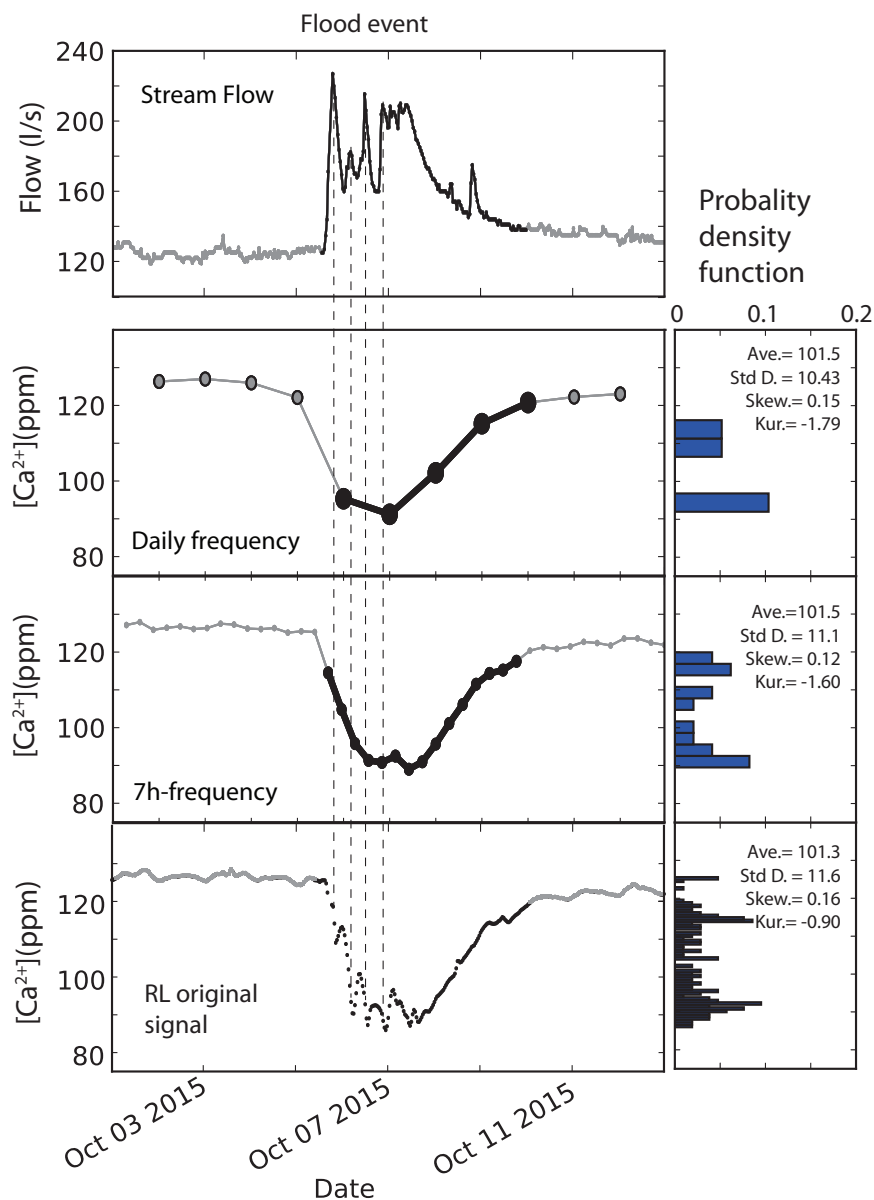




Figure 6

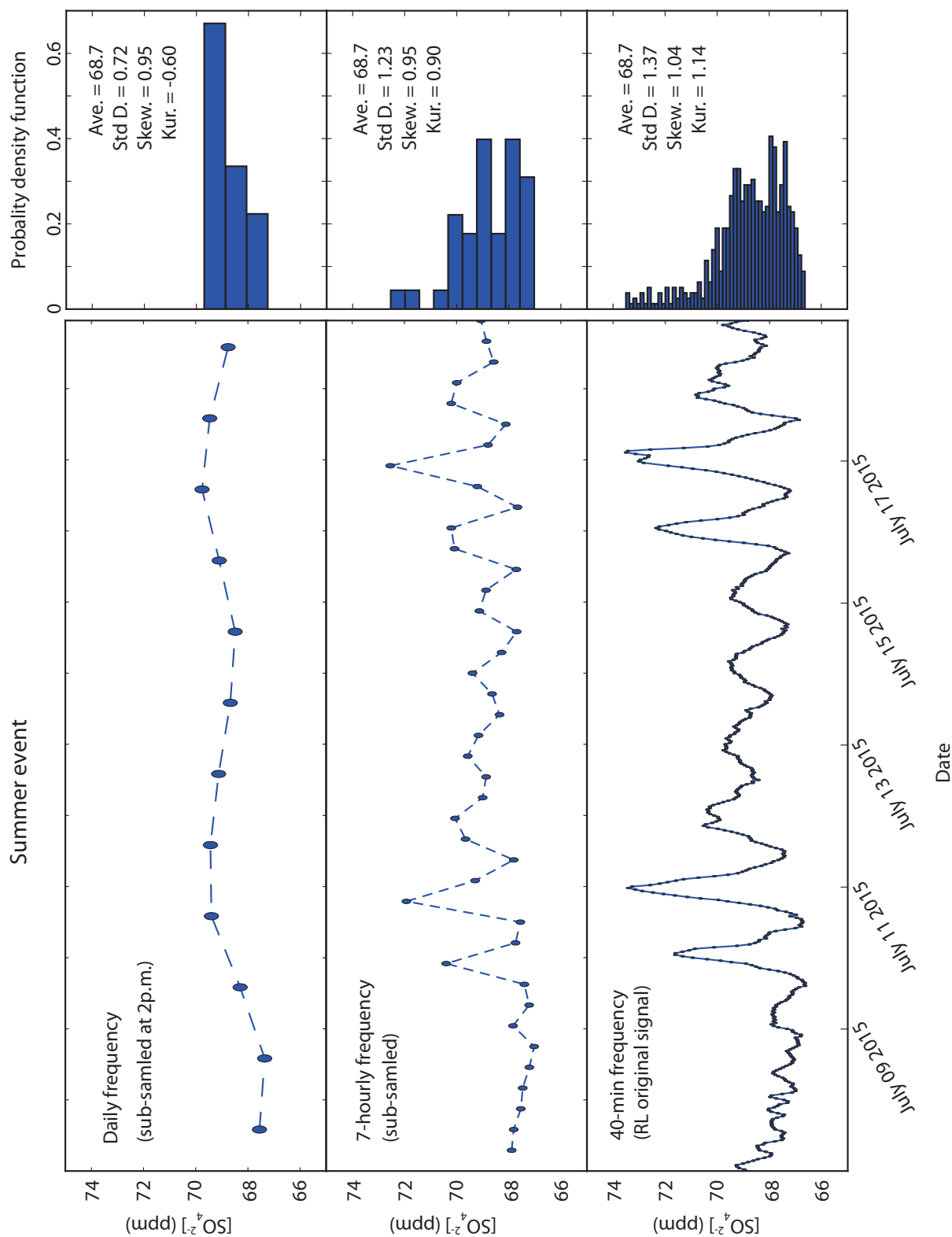




Figure 7

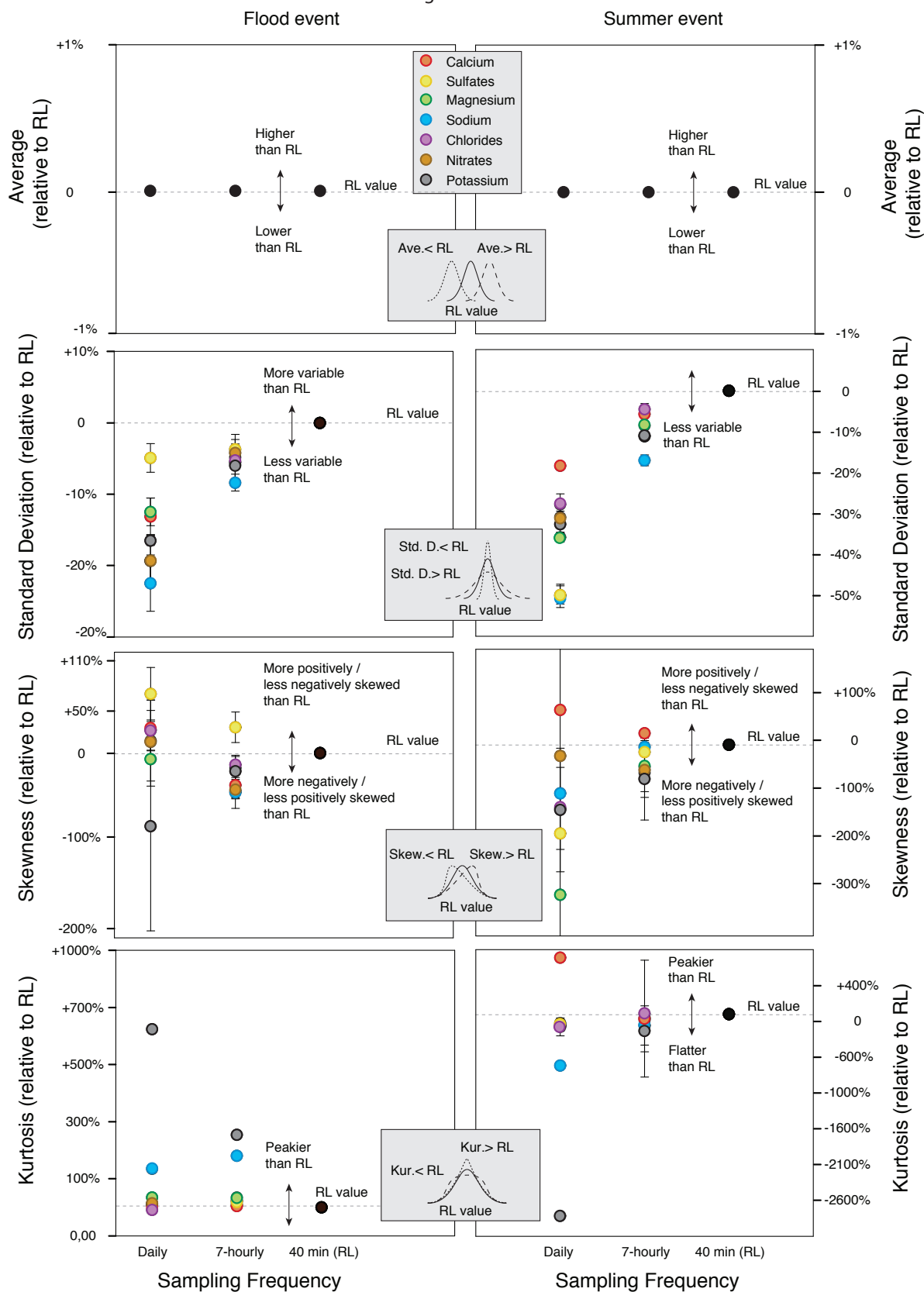




Figure 8

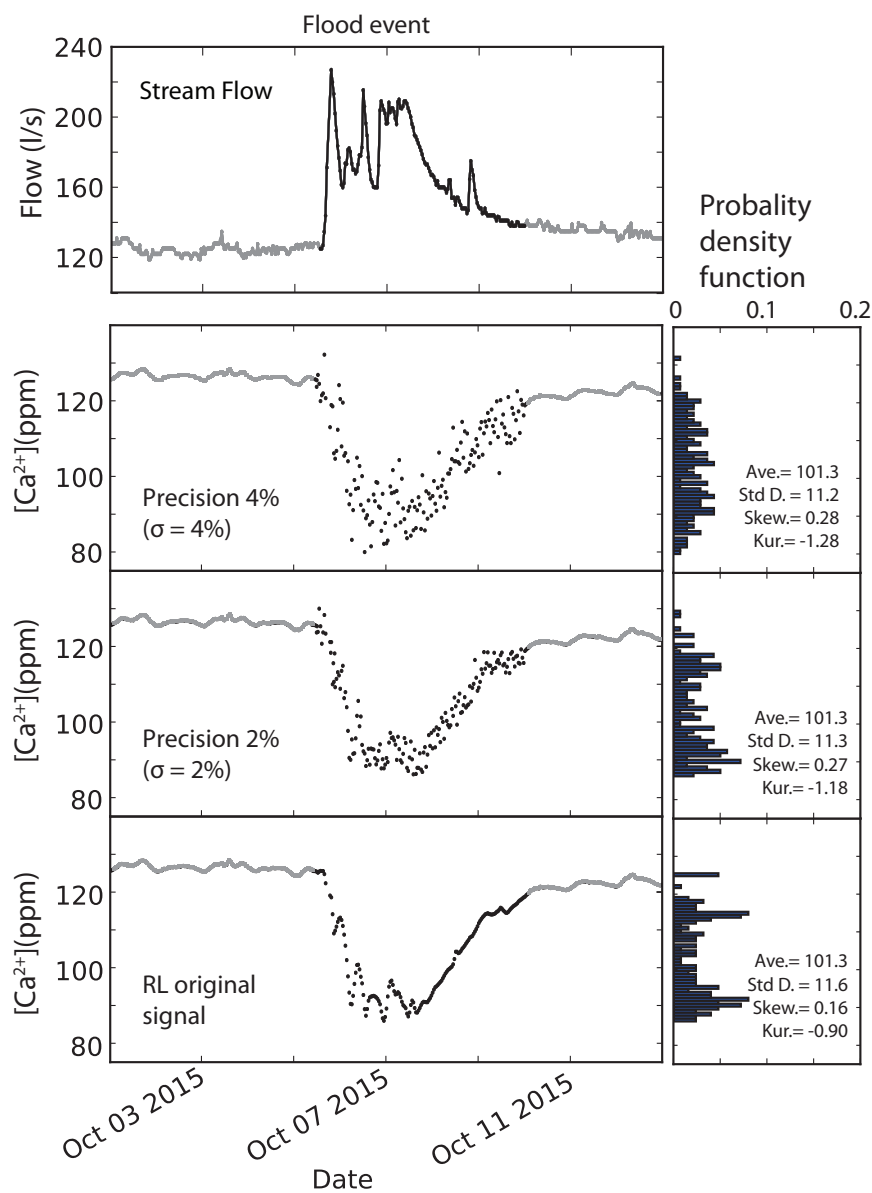




Figure 9

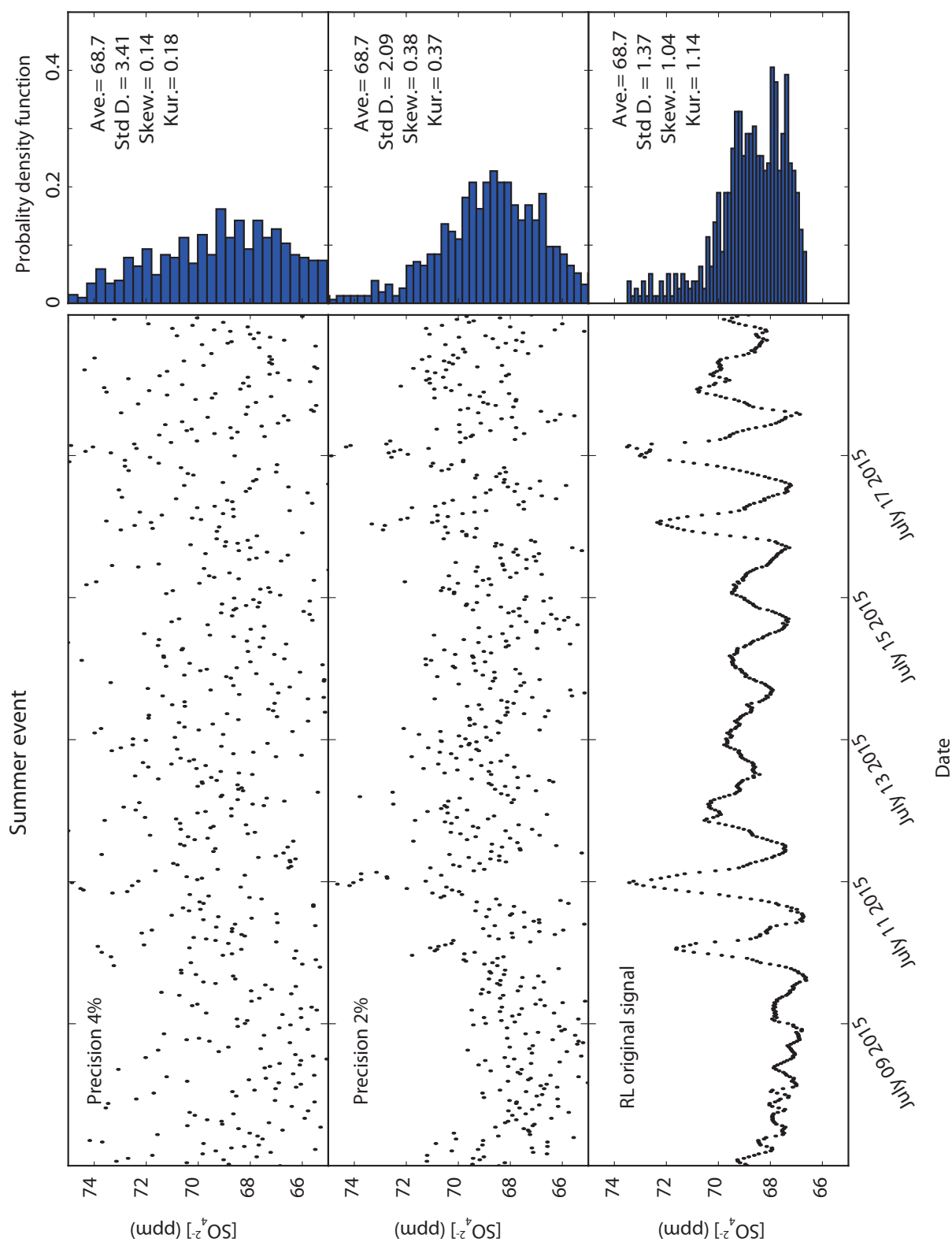
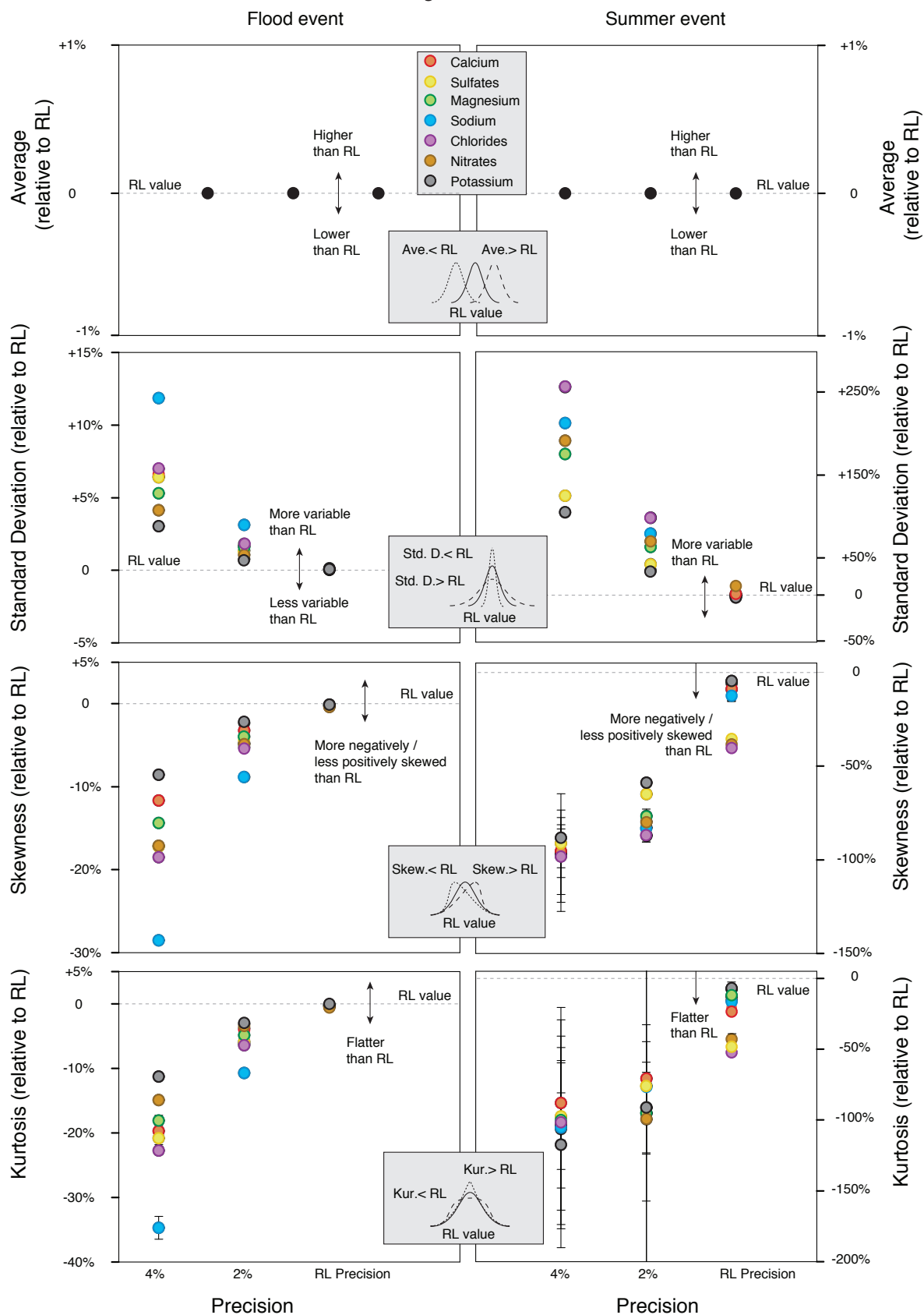




Figure 10





	Mg ²⁺	K ⁺	Ca ²⁺	Na ²⁺	SO ₄ ²⁻	NO ₃ ⁻	Cl ⁻
Calibration Solution	10.0	3.0	130.0	10.0	70.0	60.0	40.0
(mg.L ⁻¹)	0.03	0.01	0.39	0.03	0.84	0.84	0.28
(%)	0.3	0.45	0.3	0.3	1.2	1.4	0.7
One Measurement (Injection "River x1" solution 4 times)							
Number of measurement	(4)	(4)	(4)	(4)	(4)	(4)	(4)
Average (mg.L ⁻¹)	10.08	3.00	129.86	9.98	70.26	60.31	40.32
Std. Dev. (mg.L ⁻¹)	0.02	0.01	0.16	0.02	0.69	0.63	0.27
RSD (%)	0.16	0.27	0.12	0.21	0.86	0.74	0.33
One Week (Injection "River x1" solution every 8h)							
Number of measurement	(19)	(19)	(19)	(19)	(19)	(19)	(19)
Average (mg.L ⁻¹)	10.13	3.02	130.64	10.01	70.54	60.63	40.44
Std. Dev. (mg.L ⁻¹)	0.03	0.01	0.39	0.02	0.67	0.44	0.22
RSD (%)	0.28	0.32	0.30	0.22	0.96	0.72	0.54
Two months (Injection "River x1" solution every 2 days)							
Number of measurement	(28)	(28)	(28)	(28)	(25)	(25)	(25)
Average (mg.L ⁻¹)	10.33	3.14	134.34	10.05	70.05	62.33	40.57
Std. Dev. (mg.L ⁻¹)	0.06	0.04	0.80	0.05	1.17	0.55	0.43
RSD (%)	0.54	1.34	0.59	0.50	1.68	0.92	1.07



Date	<i>Number of measurements</i>	Mg ²⁺	K ⁺	Ca ²⁺	Na ²⁺	SO ₄ ²⁻	NO ₃ ⁻	Cl ⁻
RSD (%)								
20 th July 2015	(22)	0.17	0.90	0.21	0.22	0.39	0.47	0.24
28 th August 2015	(20)	0.32	0.63	0.31	0.36	0.20	0.25	0.19
17 th April 2016	(35)	0.38	1.20	0.17	0.31	0.31	0.38	0.30